Directed self-assembly of microscale hydrogels by electrostatic interaction

2013 Biofabrication 5 035004

(http://iopscience.iop.org/1758-5090/5/3/035004)

Biofabrication **5** (2013) 035004 (10pp) doi:10.1088/1758-5082/5/3/035004

Directed self-assembly of microscale hydrogels by electrostatic interaction

Yu Long Han[1,2,5], **Yanshen Yang**[1,2,5], **Shaobao Liu**[2], **Jinhui Wu**[3], **Yongmei Chen**[2,4], **Tian Jian Lu**[2,6] **and Feng Xu**[1,2,6]

[1] The Key Laboratory of Biomedical Information Engineering of Ministry of Education, Xi'an Jiaotong University School of Life Science and Technology, Xi'an 710049, People's Republic of China
[2] Bioinspired Engineering and Biomechanics Center, Xi'an Jiaotong University, Xi'an 710049, People's Republic of China
[3] State Key Laboratory of Pharmaceutical Biotechnology, Nanjing University, Nanjing 210093, People's Republic of China
[4] School of Science, Department of Chemistry, MOE Key Laboratory for Non-Equilibrium Synthesis and Modulation of Condensed Matter, Xi'an Jiaotong University, Xi'an 710049, People's Republic of China

E-mail: fengxu@mail.xjtu.edu.cn and tjlu@mail.xjtu.edu.cn

Received 22 February 2013
Accepted for publication 3 May 2013
Published 29 May 2013
Online at stacks.iop.org/BF/5/035004

Abstract
The unique benefit of electrostatic self-assembly of microscale components in solution is demonstrated for the first time. In particular, positive and negative treatment of poly(ethylene glycol) (PEG) facilitates a novel bottom-up assembly approach using electrostatic interaction from microgels with opposite charges. Fundamental investigations of electrostatic interaction of microgels reveal that the contact area of microgels determines the total energy of construct and thus the final patterns. The electrostatic self-assembly approach enables the fabrication of large and complex biological related structures (e.g., multi-layer spheroid) with accurate control. By the design of the microgels, the thickness and number of microgels in each layer can be controlled. Biological investigations of positive and negative treatments of PEG further prove the possibility of using this approach in tissue engineering, regenerative medicine and drug delivery.

S Online supplementary data available from stacks.iop.org/BF/5/035004/mmedia

(Some figures may appear in colour only in the online journal)

Introduction

The assembly of microscale components into designed patterns is a vital process to realize their functionality in various mechanical, electrical and biomedical areas [1–3]. Taking cellular function for example, most native tissues and organs are composed of numerous *microscale* reduplicative functional units (e.g., nephron in the kidney, islet in the pancreas and sinusoid in the liver [4]), with various cell types distributed in a well-defined three-dimensional (3D) space. The specific *microscale* microarchitecture provides necessary cell–cell interaction and cell–extracellular matrix (ECM) interaction for tissue-specific cellular function [5, 6]. Thus, it is essential to assemble cells *or cell-laden microgels* (*microscale components*) into such microarchitecture for the regeneration of functional tissues *in vitro* [7]. However, it is challenging to employ the conventional technique of pick-and-place robotic assembly to manipulate microscale components in an efficient manner, especially for soft materials (e.g., cells and hydrogels). The convergence of microscale technologies and hydrogel leads to novel bottom-up methods for building microscale

[5] Authors contributed equally to this work.
[6] Authors to whom any correspondence should be addressed.

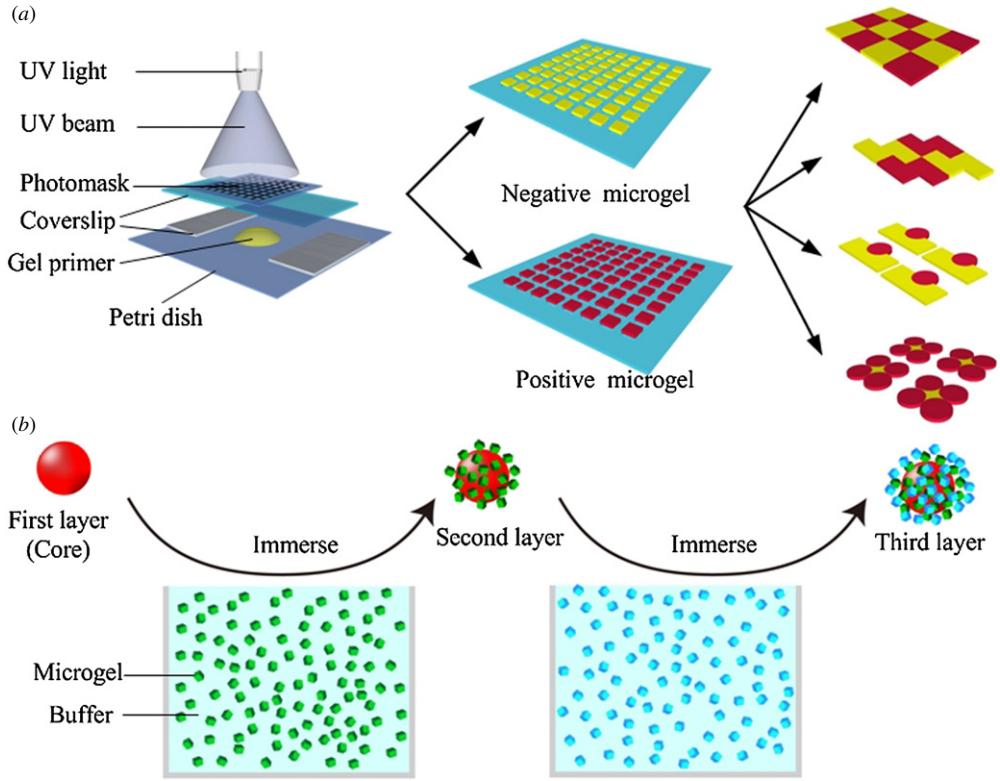

Figure 1. Schematic of self-assembly of charged microgels. (*a*) Fabrication of charged microgels using photolithography and self-assembly of microgels by electrostatic interaction; (*b*) three-dimensional assembly of microgels into multilayer spheroid constructs. The assembled construct was immersed into opposite charged microgel colloid repeatedly to form multilayer constructs.

hydrogels (i.e., microgels) and assembling these microgels into large constructs with designed microarchitecture [8].

Various methods have been developed for assembling microgels [8, 9], such as random assembly, physical manipulation and directed assembly. However, there are several challenges associated with these methods. For instance, random assembly and physical manipulation suffer from limited control and low efficiency of assembly process. Although the method based on hydrophobic effect driving force offers improved assembly efficiency, assembling complex 3D structures with this method is challenging [10]. More recently, magnetic and acoustic assembly methods are the most intriguing approaches to assemble microgels into 3D multilayer structures [11–13]. However, the magnetic force and acoustic wave may decay along hydrogel thickness, limiting the final size and number of layers in assembled 3D constructs. Thus, there is still an unmet need for a method that enables assembling microgels into large constructs in an efficient way.

Electrostatic interaction, arising from the forces that electric charges exert on each other and a common phenomenon in daily life, has been widely used in various applications. For instance, electrostatic interaction has been used for self-assembly of *nanoscale particles* to fabricate two-dimensional (2D) and 3D periodic structures [14–16]. Recently, electrostatic interaction has also been used for self-assembly of microscale particles (e.g., Nylon and Teflon) into controlled lattice structure for investigation of crystallization [17]. However, electrostatic-driven assembly of microscale soft materials in solution has not been reported, which could benefit the applications that need microscale components such as tissue engineering. These self-assembly methods based on electrostatic interaction offer several advantages such as high assembly efficiency, high potential to be scaled-up and easy control over final constructs, holding great promise to be used as bottom-up methods for *microscale* soft materials.

Hydrogels with electrostatic potential (i.e., charged hydrogels) are one of the most intelligent materials [18] and have shown great biological effect [19], promising for applications in biomedicine. For instance, a negatively charged hydrogel, PNaAMPS (poly(2-acrylamido-2-methyl- propane sulfonic acid sodium salt)), has been found to be able to enhance the adhesion, proliferation and platelet compatibility of endothelial cells [20]. However, electrostatic interaction-based self-assembly of microgels using charged hydrogels has not been explored yet.

Here, we present the first attempt to assemble microgels into 2D and 3D constructs using electrostatic interaction of hydrogels (figure 1). Firstly, PEG-based hydrogels with cationic and anionic comonomers are produced. We used poly(ethylene glycol) (PEG) due to its good mechanical and biocompatible properties and we selected two common charged hydrogels as examples, i.e., positive poly(2-(methacryloyloxy) ethyltrimethylammonium chloride) (PMETAC) and negative PNaAMPS. By copolymerizing PEG with charged hydrogels PMETAC and PNaAMPS using photolithography, we generated electrostatic potential on the surface of microgels. Then, in the presence of microgels with

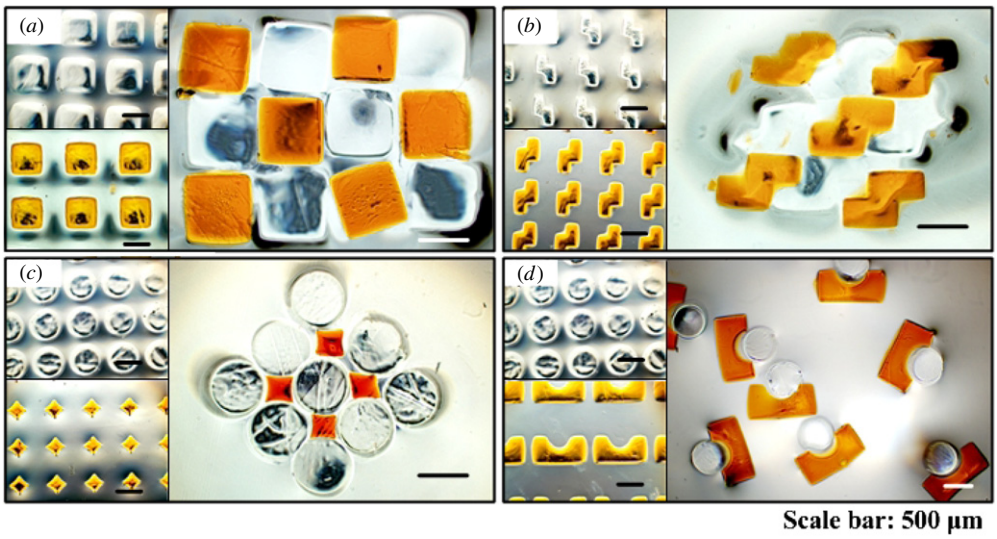

Figure 2. Self-assembly of charged microgels into different two-dimensional patterns. The microgels were designed to assemble into different patterns in a petri dish. Negatively (transparent) and positively (orange) charged square microgels (*a*); Z-shaped Tetris blocks (*b*); diamond and circle microgels (*c*); and lock-and-key microgels (*d*) were assembled into compacted 2D constructs.

opposite charges, these microgels self-assembled into pre-specified 2D constructs in an organized manner (figure 1(*a*)). By repeatedly immersing hydrogels into solution with opposite charged microgels, we assembled microgels into 3D multi-layer constructs (figure 1(*b*)). The experimental and theoretical results indicated that the electrostatic interaction of microgels is of importance to the assembly process, and the design of microgels is the main determinant factor. From a biological viewpoint, biocompatibility of charged microgels was also evaluated.

Materials and methods

Materials

2-(Methacryloyloxy) ethyltrimethylammonium chloride (METAC) was purchased from Alfa Aesar (Tianjin, China). To obtain 2-acrylamido-2-methyl-propane sulfonic acid sodium salt (NaAMPS), 2-acrylamido-2-methyl-propane sulfonic acid (Energy Chemical, Shanghai, China) was neutralized with sodium hydroxide in ethanol, which was then purified by recrystallization from acetone. Poly (ethylene glycol)dimethacrylate (PEGDA, MW 1000) was purchased from Sigma-Aldrich (St. Louis, MO). 2-Hydroxy-2-methylpropiophenone was supplied by Tokyo Chemical Industry Co., Ltd (Shanghai, China). Dulbecco's Modified Eagle Medium (DMEM), fetal bovine serum (FBS), trypsin, penicilin and streptomycin were obtained from Thermo Scientific HyClone (Logan, UT). 3-(Tri-methoxysilyl)-propyl-methacrylate (TMSPMA) was acquired from Aladdin (Shanghai, China). Live/dead cell viability kit was purchased from Invitrogen Corporation (Carlsbad, CA).

Preparation of hydrogel precursor solution

Both positively charged and negatively charged microgels were fabricated by photolithography. Positively charged hydrogel precursor solution was prepared by dissolving (10% wt/vol) PEGDA, 2-hydroxy-2-methylpropiophenone photoinitiator (0.5% wt/wt) and varying concentrations (5% and 10% wt/vol) of METAC in water. To better visualize the assembly process, we added orange food dye (2% vol/vol) in positively charged microgels in 2D assembly. Negatively charged hydrogel precursor solution was prepared by dissolving (10% wt/vol) PEGDA, 2-hydroxy-2-methylpropiophenone photoinitiator (0.5% wt/wt) and varying concentrations (5% and 10% wt/vol) of NaAMPS in water.

Fabrication of microgels

To fabricate microgels, we added a drop of hydrogel precursor solution (75 μL) on a lid of petri dish and covered it with a cover slip (figure 1(*a*)). The microgel thickness (i.e., height between petri dish and cover slip) was adjusted by the number of spacers, where we used cover slip (thickness 150 μm) as the spacer. A photo mask with defined pattern (square, lock-and-key, roundness, star and Z-shaped Tetris blocks) was put on the cover slip. The positively and negatively charged microgels were crosslinked by exposing to 365 nm UV light (1.94 mW cm^{-2}, model XLE-1000 A/F, Spectroline, USA) for 40 and 15 s, respectively. These parameters were obtained after optimization based on crosslinking of the hydrogels. The microgels were collected by gently scraping off from the cover slip and immersed into deionized (DI) water. As shown in figure S1 (supplementary information available at stacks.iop.org/BF/5/035004/mmedia), we designed square microgels with three different sizes, 200 $\times$ 200 $\times$ 300 μm^3, 400 $\times$ 400 $\times$ 300 μm^3, 500 $\times$ 500 $\times$ 300 μm^3, which were denoted as 200, 400, 500 μm microgels, respectively. We designed lock-and-key microgels, where the lock microgel was a 1000 μm $\times$ 500 μm rectangle eradicate with half of a 500 μm circle and the key microgel was a 500 μm circle. We designed diamond and circle microgels, where the circle

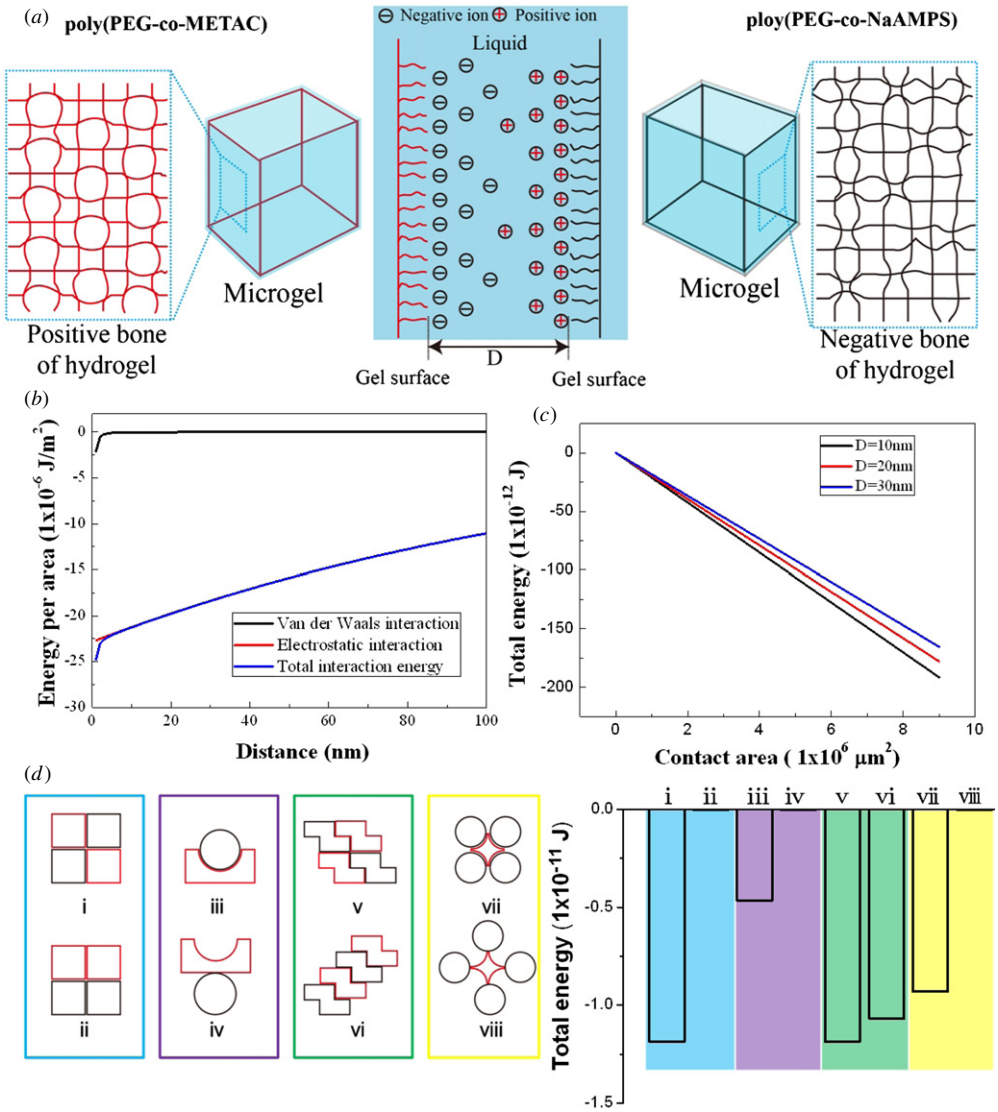

Figure 3. Theoretical analysis of various factors affecting self-assembly. (*a*) Schematic of electrostatic interaction. The porous charged microgels form an electrical double layer in liquid and exert an electrostatic fore between microgels; (*b*)–(*c*) interaction energy between microgels. Considering van der Walls interaction and electrostatic interaction, the total interaction energy is proportional to the distance (*b*) and contact area (*c*) between two microgels; (*d*) analysis of the interaction energy of different patterns observed in experiments. i, iii, v, vii were simplified patterns observed in experiments, while ii, iv, vi, viii were corresponding possible patterns.

microgels were 500 μm in diameter. We designed Z-shaped Tetris blocks, each composed of four 200 μm squares.

Zeta potential measurement and swelling test

To check the electrostatic state of synthesized hydrogels, bulk gel (about 1 cm^3) was stirred into small particles and the zeta potential of microgels was measured by Malvern Zetasizer ZS90. To test the swelling properties of charged hydrogels, we immersed the microgels in DI water after crosslinking and tracked the changes of microgel size by phase contrast imaging at different time points ($t = 0$, 5, 15, 20, 25 and 30 min) using an inverted fluorescence microscope microscopy (Olympus IX 81). The change of size was quantified by analysing the images using ImagePro Plus (IPP, version 6.0).

Assembly of 2D constructs

To assemble microgels into 2D constructs, we put hundreds of microgels with opposite charges into a thin layer of DI water in a petri dish using a pipette and gently shaked the petri dish for mixing. The final constructs were imaged by IX 81.

Theoretical analysis

Considering the electric charges of hydrogels were probably caused by the counter-ion condensation effect [21, 22], here we used the DLVO theory to simulate the interaction energy of charged microgels [23]. The schematic illustration presented in figure 3(*a*) describes two charged surfaces interacting with each other through a liquid medium. The interacting force is affected by the electrostatic interaction due to the so-called electrical double layer (EDL) of counter-ions and

van der Waals interaction. The interaction energy per unit area due to van der Waals interaction between two surfaces can be calculated as

$$W(D)_{A_1} = -\frac{A}{12\pi D^2} \quad (1)$$

where D is the distance between two surfaces, and A is the Hamaker constant given as

$$A = \pi^2 C \rho_1 \rho_2 \quad (2)$$

Herein, ρ_1 and ρ_2 denote separately the number of atoms per unit area in the two interacting surfaces and C is the coefficient in particle–particle pair interaction. The electrostatic interaction energy per unit area between two planar surfaces due to EDL can be calculated as

$$W(D)_{A_2} = -\left(\frac{64 k_B T \rho_\infty \gamma_1 \gamma_2}{\kappa}\right) \mathrm{e}^{-\kappa D} \quad (3)$$

where k_B is the Boltzmann constant, and γ_i is the reduced surface potential:

$$\gamma_i = \tan\ h\left(\frac{ze\varphi_{0i}}{4k_B T}\right), \quad i = 1,\ 2 \quad (4)$$

Herein, φ_{0i} is the potential on surfaces 1 and 2; $1/\kappa$ is the thickness of the diffuse electric double layer, which is known as the Debye screening length, with:

$$\kappa = \left(\sum_i \rho_{\infty i}\, \mathrm{e}^2 z_i^2 / \varepsilon\varepsilon_0 k_B T\right)^{1/2} \quad (5)$$

$\rho_{\infty i}$ is the number density of ion i in the bulk solution; z is the valency of the ion; ε_0 is the electric constant, ε is the relative static permittivity; and T is absolute temperature.

Combining van der Waals interaction energy with electrostatic interaction energy, the interaction between two surfaces in a liquid can be expressed as:

$$W(D) = W(D)_{A_1} + W(D)_{A_2} \quad (6)$$

Finally, the total free energy between two microgels with interaction area S is obtained as:

$$E_{\text{free\_total}} = W(D)S \quad (7)$$

The parameters we used in the calculation are listed in table S1 (supplementary information available at stacks.iop.org/BF/5/035004/mmedia).

Assembly of 3D constructs

To assemble 3D multilayer constructs, a droplet of negatively charged microgel precursor (6 μL) was first formed on a wire due to surface tension (with diameter of 2 mm) as a core. After crosslinking, we put the negatively charged core into liquid containing positively charged microgels to assemble the second layer and then into liquid with negatively charged microgels to assemble the third layer (figure 1(*b*)). This process was repeated to assemble further layers. The assembled constructs can be further stabilized by exposing to UV light for several seconds. To better visualize each layer in the assembled constructs, we used three-layer constructs as an example and stained each layer with different fluorescent dyes (rhodamine B for first layer, FITC for second layer and DAPI for third layer), which was observed under IX 81.

To quantify the 3D assembly process, we used two-layer constructs as a model system to study the layer thickness and numbers of building blocks as a function of the building block dimensions (figures 4(*c*) and (*d*)), which were assembled following the process described above. The diameters of the core and the assembled two-layer spheroid were measured by analysing the photos using IPP, which was used to calculate the thickness of the second layer. The microgels in the second layer were intensely washed down by PBS and the number was counted under microscopy.

To check the decay of electrostatic interaction, we fabricated a seven-layer spheroid which was difficult to achieve through other methods suffering from force decay. The assembly process is the same as described above. After the assembly of each layer, the diameter was measured under microscopy.

Cell encapsulation and cell viability test

We used NIH-3T3 fibroblasts as a model cell system in this study. The cells were cultured in DMEM supplemented with FBS (10% vol/vol) and penicillin-streptomycin (1% vol/vol) in standard cell culture condition (humidified, 5% CO_2). The cells were trypsinized when confluent and resuspended in hydrogel precursor (*PEGDA*, 10%, *photoinitiator,* 0.05% *and PNaAMPS or PMETAC* 5%, 10%) prepared with DMEM culture medium (instead of DI water) *that was sterilized via filtration* (0.22 μm *pore size*). The final cell concentration for viability test was 1×10^7 cells mL^{-1}. Then the cell-laden microgels were fabricated using the method described above. Upon crosslinking, the microgels were immersed into culture medium. Cell availability was tested immediately after crosslinking and also at the time point of 24 and 48 h after crosslinking by live/dead staining. Live/dead staining was done following the product protocol. Cell-laden microgels were incubated with lived/dead dyes for 30 min and imaged using IX 81. Cell viability was assessed by analysing the images using IPP.

Statistical analysis

All the experiments were repeated at least three times. The data are shown as mean $\pm$ standard deviation.

Results and discussion

To test electrostatic interaction of charged microgels, we first assembled microgels into 2D constructs. For this, we synthesized negatively charged ploy(PEG-co-NaAMPS) and positively charged poly(PEG-co-METAC) microgels with different shapes (square, lock-and-key, roundness, star and Z-shaped Tetris blocks) by photolithography (figure 1 and figure S1, available at stacks.iop.org/BF/5/035004/mmedia). The zeta potential of microgels was -38.7 ± 5.5 mV and 30.9 ± 2.8 mV, respectively. After mixing microgels with opposite charges, the microgels were driven by electrostatic attraction and we observed that the microgels assembled into compacted constructs (figure 2). Similar phenomenon has also

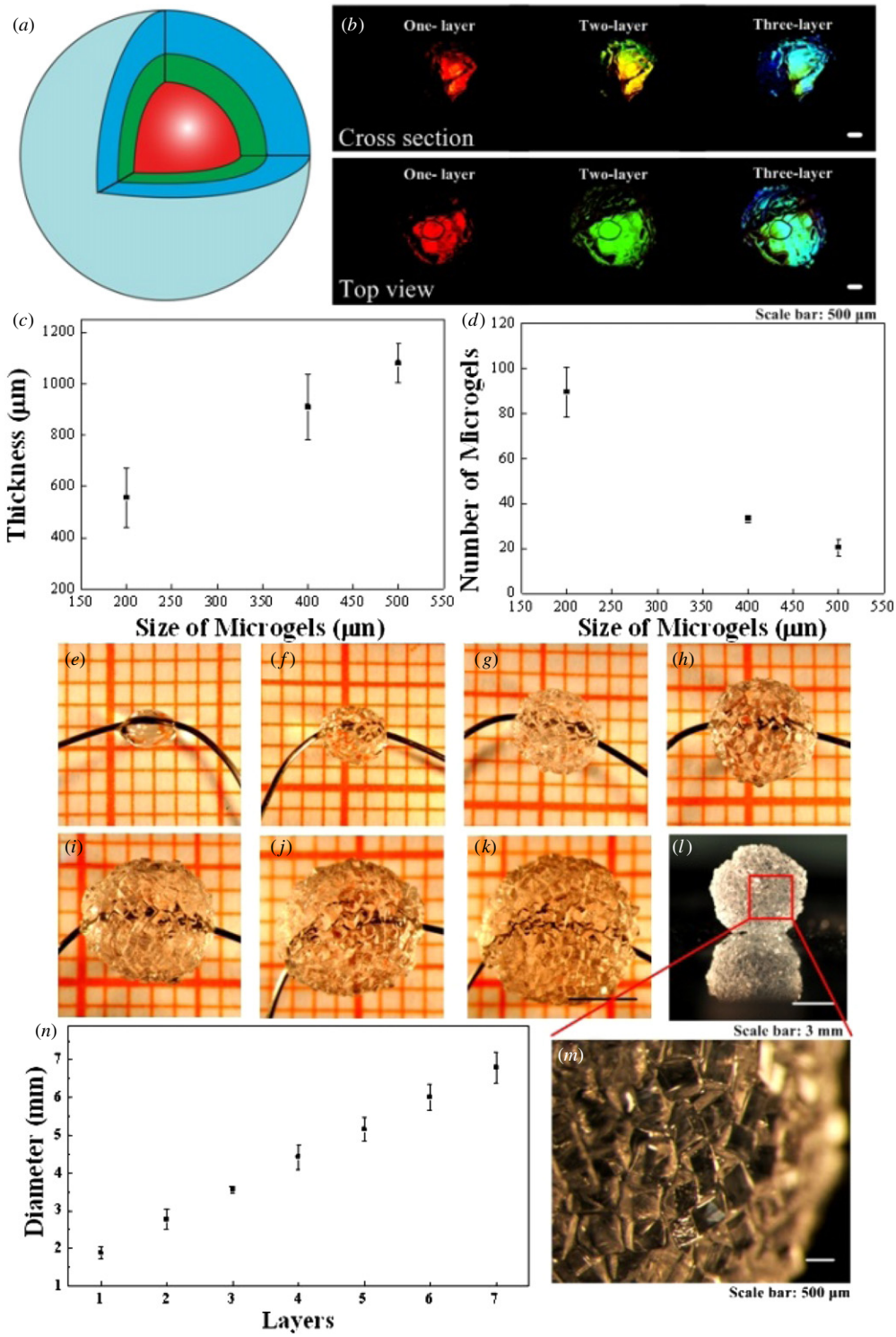

Figure 4. Self-assembly of complex 3D constructs. (*a*) Schematic of three-layer spheroid construct; (*b*) merged fluorescent photos of three-layer spheroid in cross section view and top view. The first, second and third layer were stained with rhodamine B, FITC and DAPI, respectively; (*c*)–(*d*) quantified 3D assembly process by thickness (*c*) and number of microgels (*d*); (*e*)–(*n*) assembly and quantification of seven-layer spheroid. The construct was assembled layer by layer (*c*)–(*k*); after assembly the construct was removed from iron wire (*l*)–(*m*); The diameter of the construct was quantified layer by layer (*n*).

been observed in the directed assembly approach in which case the surface tension drives microgels maximizing the contact area between microgels [10]. We have further shown the control over 2D construct of our method by fabricating more complex 2D patterns (e.g., lock and key, figure 2(*d*)) and high ordered patterns (e.g., square and Z-shaped Tetris blocks, figures 2(*a*)–(*b*)). To eliminate the effect caused by physical confinement resulting from matching shapes, we performed experiments with neurally charged hydrogels (i.e., 10% PEG), and we do not find any assembled cases (figure S3, available at

stacks.iop.org/BF/5/035004/mmedia), indicating the physical confinement is not the major cause.

To better understand the interplay of electrostatic microgels underlying the assembly process, we proposed a theoretical model to analyse the total interaction energy of the assembly system (figure 3). Generally, thermodynamic equilibrium theory can be used to describe the process of self-assembly, where the final organized structures should have minimized system free energy [24]. Here, we considered van der Waals interaction energy and electrostatic interaction energy for a system with two planar surfaces, in which case the total energy per unit area depends on the distance between the two surfaces, figure 3(*b*). Although it is challenging to measure precisely the distance and the force between two microgels, it has been reported that the force was maximized at the distance of 30 nm and almost lost at a distance of 500 nm during the assembly of nanoparticles by electrostatic interaction [16]. It is worth noting that in a few experimental situations (such as figure 2(*d*)) the distance between two surfaces of microgel is obviously bigger than nanoscale. We speculated the final configuration of construct is the balance of electrostatic interaction and physical confinement, where electrostatic attraction makes them compact while physical confinement plays as an obstructer. Besides, the electrostatic attraction between contacting points of two surfaces also prevent further movement. This phenomenon indirectly proved that the electrostatic force is strong enough to keep the construct stable even if the two surfaces are not entirely in contact. To confirm the electrostatic interaction between microgels, we used a negatively charged microgel to drag positively charged microgel (video 1, supplementary information available at stacks.iop.org/BF/5/035004/mmedia) while using two neurally charged microgels (i.e., PEG) as control (video 2, supplementary information available at stacks.iop.org/BF/5/035004/mmedia). The results indicated that electrostatic interaction plays a major role in the assembly process and the attraction is strong even though the two surfaces of microgels are not well contacted. Here, we chose three distances between two microgel surfaces (i.e., 10, 20 and 30 nm) and neglected the force resulting from hydrogels inside. Briefly, the total energy increased with the distance, e.g., the total energy is -21.27×10^{-6}, -19.76×10^{-6} and -18.38×10^{-6} J m^{-2} for surface–surface distance of 10, 20 and 30 nm, respectively. For all of these cases, electrostatic interaction energy is much larger than van der Waals interaction energy, indicating its important role in the assembly process (figure 3(*b*)). To calculate the total energy of the assembled construct, we analysed the relationship between total interaction energy (E) and contact area at three surface–surface distances (i.e., 10, 20 and 30 nm), and found proportional relationship between total energy and contact area (figure 3(*c*)). Since the system will stabilize in a state with minimized energy [25], the assembly process has a tendency to minimize the contact area. We compared the total energy between different patterns used in our experiments (figure 3(*d*)), which explains the phenomenon we observed in figure 2. For instance, the resulting pattern for the case of Z-shaped Tetris microgels assembly (figure 3(*d*)v) had a lower total energy than other possible patterns (figure 3(*d*)vi), which was -1.19×10^{-11} J for figure 3(*d*)v and -1.07×10^{-11} J for figure 3(*d*)vi.

Besides the contact area of microgels, another important factor that affects assembly process is the ionic strength which significantly affects Debye length thus electrostatic interaction. Therefore, the electrostatic interaction is sensitive to solution compositions, offering advantages for reversing assembly by changing ionic concentration. Our previous studies shown that the negatively charged hydrogels can absorb the proteins in culture medium (with FBS), which may neutralize the charges on the surface and reduce the electrostatic attraction force. To address this challenge, we propose to assemble microgels in PBS solution which is a standard buffer solution usually used for cell culture. Although the electrostatic attraction force was reduced in PBS, it still can drag microgels (video 3, supplementary information available at stacks.iop.org/BF/5/035004/mmedia), indicating its potential for tissue engineering applications.

To evaluate the capability of electrostatic approach for fabricating complex constructs, we assembled microgels into 3D multi-layered spheroid (figures 4(*a*)-(*b*)). To quantify the 3D assembly process, we measured the thickness of each layer (figure 4(*c*)) and counted the number of microgels (figure 4(*d*)) for assembly using different sized microgels in a two-layer construct. The numbers of microgel were 89 $\pm$ 11, 33 $\pm$ 2 and 20 $\pm$ 4 for microgel with size of 200, 400 and 500 μm, respectively. Meanwhile, the thickness of the assembled second layer also depended on the size of microscale hydrogels, which were 554.5 $\pm$ 115.8, 908.3 $\pm$ 125.8 and 1078.6 $\pm$ 75.5 μm for three different sized microgels. Due to microgel swelling, the thickness is larger than microgel sizes (figure S2, supplementary information available at stacks.iop.org/BF/5/035004/mmedia). By adjusting the size of microgels in each layer in our method, we can control the distribution of microgels in each layer and between different layers, which is beneficial to the control over both microarchitecture and 3D macro-features. Such capability is important for several applications, tissue engineering in particular. For instance, millions of islets in spheroid shape are distributed through whole pancreas in a specific pattern [26], while alpha, beta and delta cells are distributed within the islet with certain spatial positions [27]. In the assembled construct, the orientation of microgels in layer is another important factor to determine structural quality. According to the theoretical analysis, the electrostatic force between two microgels tends to maximize the contact area. However, in the 3D assembly process, the final orientation of microgels is also affected by the complex 3D physical confinement. Thus it is technically difficult to control the orientation of microgels in the layer using the current procedure. We envision that this problem could be solved by the design of microgels with high length-width ratio. Besides, the developed assembly method relies on electrostatic force exerting between assembled unites (i.e., microgels) instead of external forces, e.g., surface tension and capillary force in liquid–liquid surface [10], liquid–solid surface [28], and liquid–air surface [29] directed assembly

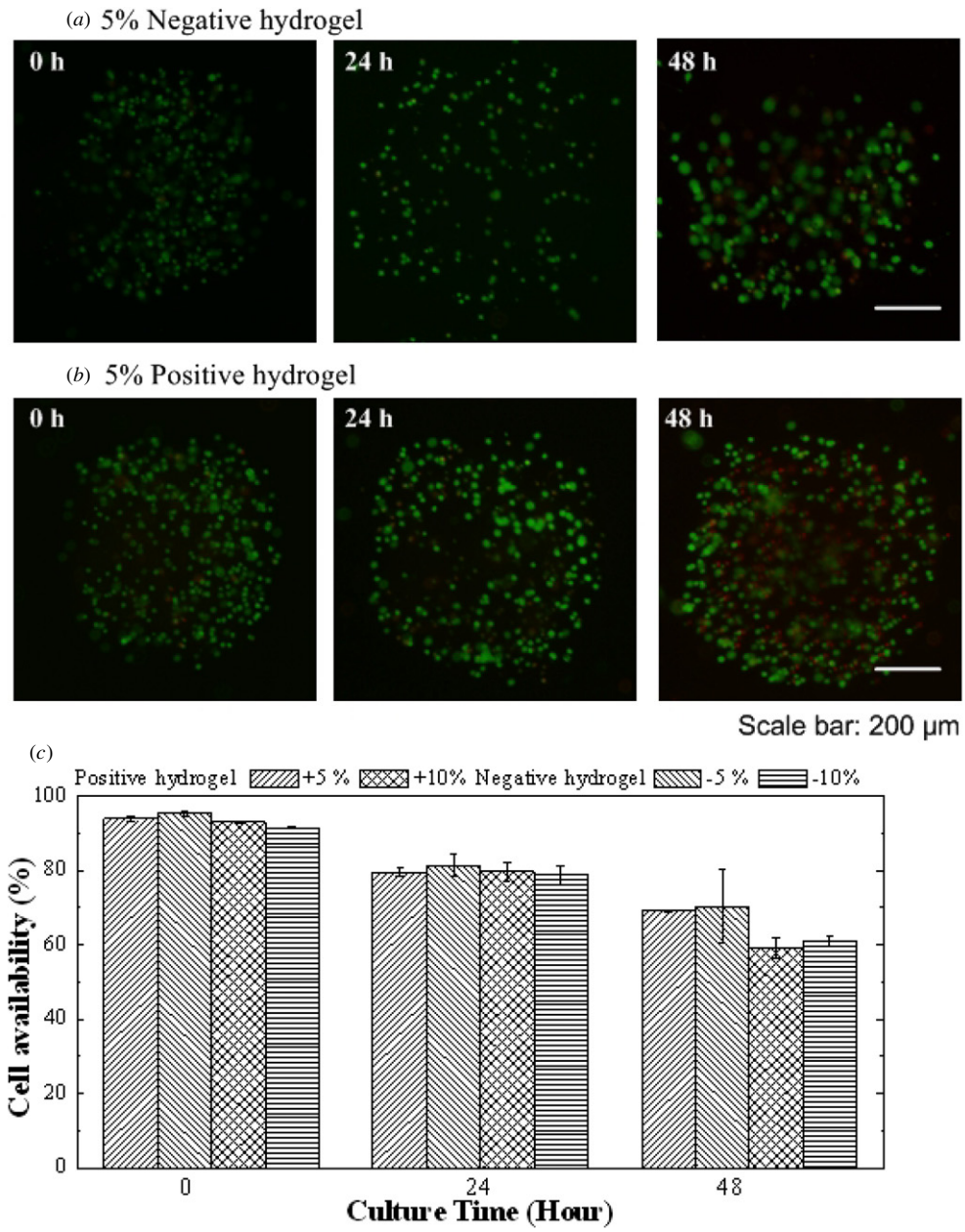

Figure 5. Cell availability. (*a*), (*b*) Live/dead stain florescent images of cells encapsulated in 5% charged microgels immediately after crosslinking and at the point of 24 and 48 h after crosslinking; (*c*) quantified availability of cells encapsulated in charged microgels.

approaches. This would significantly reduce the dependence on environments, e.g., properties of liquid and solid surface that are the main effective factors in other directed assembly methods, and improve the ability and efficiency to achieve assembled patterns in high ordered manner.

To test the decay of electrostatic force with increasing number of assembly layers and the ability of electrostatic approach to form large constructs, we assembled seven-layer spheroids (figures 4(*e*)–(*l*)). The diameter of the spheroid increased with increasing number of assembly layers (figure 4(*n*)) and could achieve as large as 6.8 ± 0.4 mm when seven layers were assembled using 400 μm sized microgels (figure 4(*m*)). This electrostatic layer-by-layer assembly method has been used for micropatterning, thin film coating [30, 31] even electronic device [32]. More recently, this approach has been applied to biomedical applications including design of synthetic hierarchy bio-structures such as yeastosome structures and to tune mechanical properties of microgels, which offers advantages of better control ability over assembly [33, 34].

In comparison with other microgel assembly methods such as magnetic and acoustic assembly, we can achieve a larger number of layers and thus larger size of final construct. In the magnetic microgel assembly approach, the maximum number of assembled layers was limited by the decay of magnetic field and the concentration of magnetic nanoparticles encapsulated in microgels. With increasing layer number, either magnetic nanoparticles with high concentration or magnetic field with high intensity are needed, which may cause cell viability issues. While

in the acoustic assembly approach, soft microgels may absorb energy significantly, making it challenging to achieve assembly of multiple layers. Compared with these two methods, the electrostatic force does not decay even after the assembly of seven layers as observed in our study, since the assembly is dependent on the electrostatic force between assembled neighbouring layers. We expect that the developed method can achieve assembly of even more layer numbers, because the electrostatic force has been used to assemble construct thousands of times larger than individual building blocks. For instance, centimetre scale membrane can be achieved by self-assembly of nanoscale molecules with opposite charges [35].

There are various existing methods to fabricate 3D cellular constructs with complex microarchitectures, e.g., cell printing [36–38], multilayer photopatterning [39] and microfabricated scaffolds [40]. Compared with these methods, the approach developed here is simple and scalable, attractive for various applications such as tissue engineering and regenerative medicine. In addition, this method could be used to fabricate other complex structures such as tube. Besides, there is no need for any other peripheral equipment such as magnetic or acoustic generator.

To check the biocompatibility of our method, we tested the effect of charged hydrogel on cells and assessed cell availability of fibroblasts encapsulated in charged hydrogels with different charge concentrations (5% and 10% positive and negative hydrogels) (figure 5). Immediately after crosslinking, there were only a few dead cells in both positively and negatively charged microgels (figures 5(*a*)-(*b*)) and the cell availability was larger than 90% (figure 5(*c*)). The radical species produced by photoinitiator may cause cell toxicity. However, such toxicity is dependent on the exposure time to UV light and photoinitiator concentration. In fact, the toxicity can be minimized by optimizing these parameters. The photoinitiator used in our study has been proved to have minimal side effect (cell death) over many cell types [41]. According to this, the side effect is negligible for the parameters used in this study as confirmed by our cell viability results. This result is consistent with previous studies reported on PEG based hydrogels [42], indicating the charged hydrogel will not significantly reduce cell viability. Although there was a decrease of cell viability with culture, it remained about 70% after 48 h within both the 5% positively and 5% negatively charged hydrogel. While the present method is applicable to a wide range of soft materials, we choose PEG because of its good mechanical and biocompatible properties. However, PEG is not biodegradable *itself* which may affect cell viability. Thus, cell availability may be improved by replacing the PEG by other biodegradable hydrogels such as collagen or gelatin based hydrogels [43]. This issue will be addressed in a separate study. Besides, lots of studies have shown that biodegradable PEG based hydrogel can be realized by proper chemical modification [44, 45], which offer another way to solve this problem.

Conclusions

In summary, we have demonstrated a general approach that utilizes the electrostatic interaction of charged soft materials to self-assemble microgels into large 2D and 3D constructs in a controlled manner. Theoretical analysis uncovered that the electrostatic interaction energy plays a vital role in the process of self-assembly and the principle of self-assembly is to maximize the contact area of microgels with opposite charges. As applied to tissue engineering, the large biological related constructs (i.e., sphere) were assembled overcoming the decay of interaction force in other methods. This direct approach may also be evolved to the indirect approach by using an external electric field, and has great potential to be scaled-up. For instance, the combination of electrode assays and charged microgels would result in a high throughput assembly. Owing to its simplicity and flexibility, we believe that the electrostatic interaction of microscale charged soft materials will have a significant impact on current bottom-up tissue engineering approaches and encourage innovation in a wide range of application areas.

Acknowledgment

This research was supported by the Major International Joint Research Program of China (11120101002), the Key Project of Chinese Ministry of Education (313045), the Projects of International Cooperation and Exchanges NSFC (2013DFG02930), the Program for New Century Excellent Talents in University (NCET-12-0437), the South Wisdom Valley Innovative Research Team Program, the China Postdoctoral Science Foundation funded project (2010-0201110040, 2013M532054), the National Natural Science Foundation of China (51173127, 51073144, 81202474) and the Natural Science Foundation of Jiangsu (BK2011572).

References

[1] Baksh M M, Jaros M and Groves J T 2004 Detection of molecular interactions at membrane surfaces through colloid phase transitions *Nature* **427** 139–41

[2] Rinne S A, Garcia-Santamaria F and Braun P V 2008 Embedded cavities and waveguides in three-dimensional silicon photonic crystals *Nature Photon.* **2** 52–6

[3] Gracias D H *et al* 2000 Forming electrical networks in three dimensions by self-assembly *Science* **289** 1170–2

[4] Costanzo L 2006 *Physiology* 3rd edn (Philadelphia, PA: Saunders)

[5] Junt T, Scandella E and Ludewig B 2008 Form follows function: lymphoid tissue microarchitecture in antimicrobial immune defence *Nat. Rev. Immunol.* **8** 764–75

[6] Mebius R E and Kraal G 2005 Structure and function of the spleen *Nat. Rev. Immunol.* **5** 606–16

[7] Griffith L G and Naughton G 2002 Tissue engineering–current challenges and expanding opportunities *Science* **295** 1009–14

[8] Nichol J W and Khademhosseini A 2009 Modular tissue engineering: engineering biological tissues from the bottom up *Soft Matter* **5** 1312–9

[9] Gurkan U A *et al* 2012 Emerging technologies for assembly of microscale hydrogels *Adv. Healthc. Mater.* **1** 149–58

[10] Du Y *et al* 2008 Directed assembly of cell-laden microgels for fabrication of 3D tissue constructs *Proc. Natl Acad. Sci.* **105** 9522–7
[11] Xu F *et al* 2011 Three-dimensional magnetic assembly of microscale hydrogels *Adv. Mater.* **23** 4254–60
[12] Xu F *et al* 2011 The assembly of cell-encapsulating microscale hydrogels using acoustic waves *Biomaterials* **32** 7847–55
[13] Li Y *et al* 2012 Magnetic hydrogels and their potential biomedical applications *Adv. Funct. Mater.* **23** 660–72
[14] Kolny J, Kornowski A and Weller H 2002 Self-organization of cadmium sulfide and gold nanoparticles by electrostatic interaction *Nano Lett.* **2** 361–4
[15] Kalsin A M *et al* 2006 Electrostatic self-assembly of binary nanoparticle crystals with a diamond-like lattice *Science* **312** 420–4
[16] Spruijt E *et al* 2011 Reversible assembly of oppositely charged hairy colloids in water *Soft Matter* **7** 8281–90
[17] Cademartiri R *et al* 2012 A simple two-dimensional model system to study electrostatic-self-assembly *Soft Matter* **8** 9771–91
[18] Eichenbaum G M *et al* 1998 pH and ion-triggered volume response of anionic hydrogel microspheres *Macromolecules* **31** 5084–93
[19] Chen Y M, Yang J J and Gong J P 2009 Adhesion, spreading, and proliferation of endothelial cells on charged hydrogels *J. Adhes.* **85** 839–68
[20] Chen Y M *et al* 2007 Platelet adhesion to human umbilical vein endothelial cells cultured on anionic hydrogel scaffolds *Biomaterials* **28** 1752–60
[21] Manning G S 1969 Limiting laws and counterion condensation in polyelectrolyte solutions I. Colligative properties *J. Chem. Phys.* **51** 924
[22] Manning G S 1975 Limiting law for the conductance of the rod model of a salt-free polyelectrolyte solution *J. Phys. Chem.* **79** 262–5
[23] Bhattacharjee S, Elimelech M and Borkovec M 1998 DLVO interaction between colloidal particles: beyond derjaguin's approximation *Croat. Chem. Acta* **71** 883–903
[24] Grzelczak M *et al* 2010 Directed self-assembly of nanoparticles *ACS Nano* **4** 3591–605
[25] Anderson V J and Lekkerkerker H N W 2002 Insights into phase transition kinetics from colloid science *Nature* **416** 811–5
[26] Sleisenger M H, Feldman M, Friedman L S and Brandt L J 2009 *Sleisenger & Fordtran's Gastrointestinal and Liver Disease: Pathophysiology, Diagnosis, Management* 9th edn (St. Louis, MO: MD Consult)
[27] Brissova M *et al* 2005 Assessment of human pancreatic islet architecture and composition by laser scanning confocal microscopy *J. Histochem. Cytochem.* **53** 1087–97
[28] Du Y *et al* 2010 Surface-directed assembly of cell-laden microgels *Biotechnol. Bioeng.* **105** 655–62
[29] Fernandez J G and Khademhosseini A 2010 Micro-masonry: construction of 3D structures by microscale self-assembly *Adv. Mater.* **22** 2538–41
[30] Mendelsohn J D *et al* 2002 Rational design of cytophilic and cytophobic polyelectrolyte multilayer thin films *Biomacromolecules* **4** 96–106
[31] Elbert D L, Herbert C B and Hubbell J A 1999 Thin polymer layers formed by polyelectrolyte multilayer techniques on biological surfaces *Langmuir* **15** 5355–62
[32] Ho P K H *et al* 2000 Molecular-scale interface engineering for polymer light-emitting diodes *Nature* **404** 481–4
[33] Chang Y-W *et al* 2012 Uniform yeast cell assembly via microfluidics *Biomicrofluidics* **6** 024118
[34] Luo D *et al* 2007 Cell encapsules with tunable transport and mechanical properties *Biomicrofluidics* **1** 034102
[35] Capito R M *et al* 2008 Self-assembly of large and small molecules into hierarchically ordered sacs and membranes *Science* **319** 1812–6
[36] Mironov V, Kasyanov V and Markwald R R 2011 Organ printing: from bioprinter to organ biofabrication line *Curr. Opin. Biotechnol.* **22** 667–73
[37] Xu F *et al* 2011 A three-dimensional in vitro ovarian cancer coculture model using a high-throughput cell patterning platform *Biotechnol. J.* **6** 204–12
[38] Xu F *et al* 2011 Embryonic stem cell bioprinting for uniform and controlled size embryoid body formation *Biomicrofluidics* **5** 022207
[39] Tsang V L *et al* 2007 Fabrication of 3D hepatic tissues by additive photopatterning of cellular hydrogels *FASEB J.* **21** 790–801
[40] Liu Tsang V and Bhatia S N 2004 Three-dimensional tissue fabrication *Adv. Drug Deliv. Rev.* **56** 1635–47
[41] Williams C G *et al* 2005 Variable cytocompatibility of six cell lines with photoinitiators used for polymerizing hydrogels and cell encapsulation *Biomaterials* **26** 1211–8
[42] Huang G *et al* 2012 Cell-encapsulating microfluidic hydrogels with enhanced mechanical stability *Soft Matter* **8** 10687–94
[43] Rafat M *et al* 2008 PEG-stabilized carbodiimide crosslinked collagen–chitosan hydrogels for corneal tissue engineering *Biomaterials* **29** 3960–72
[44] Kloxin A M, Tibbitt M W and Anseth K S 2010 Synthesis of photodegradable hydrogels as dynamically tunable cell culture platforms *Nat. Protoc.* **5** 1867–87
[45] Kloxin A M *et al* 2009 Photodegradable hydrogels for dynamic tuning of physical and chemical properties *Science* **324** 59–63